JACS
JOURNAL OF THE AMERICAN CHEMICAL SOCIETY

Article

pubs.acs.org/JACS

A Cyanine-Modified Nanosystem for *in Vivo* Upconversion Luminescence Bioimaging of Methylmercury

Yi Liu, Min Chen, Tianye Cao, Yun Sun, Chunyan Li, Qian Liu, Tianshe Yang, Liming Yao, Wei Feng, and Fuyou Li*

Department of Chemistry and The State Key Laboratory of Molecular Engineering of Polymers and Institute of Biomedicine Science, Fudan University, Shanghai, 200433, P. R. China

Supporting Information

ABSTRACT: Methylmercury ($MeHg^+$) is a strong liposoluble ion, which can be accumulated in the organs of animals and can cause prenatal nervous system and visceral damage. Therefore, the efficient and sensitive monitoring of $MeHg^+$ in organisms is of great importance. Upconversion luminescence (UCL) detection based on rare-earth upconversion nanophosphors (UCNPs) as probes has been proved to exhibit a large anti-Stokes shift, no autofluorescence from biological samples, a remarkably deep penetration depth, and no photobleaching. In this study, a hydrophobic heptamethine cyanine dye (hCy7) modified by two long alkyl moieties and amphiphilic polymer (P-PEG)-modified nanophosphors (hCy7-UCNPs) was fabricated as a highly sensitive water-soluble probe for UCL monitoring and bioimaging of $MeHg^+$. Further application of hCy7-UCNPs for sensing $MeHg^+$ was confirmed by an optical titration experiment and upconversion luminescence live cell imaging. Using the ratiometric upconversion luminescence as a detection signal, which provides a built-in correction for environmental effects, the detection limit of $MeHg^+$ for this nanosystem was as low as 0.18 ppb. Importantly, the hCy7-UCNPs nanosystem was shown to be capable of monitoring $MeHg^+$ *ex vivo* and *in vivo* by upconversion luminescence bioimaging.

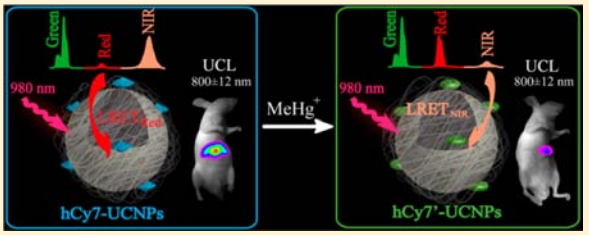

INTRODUCTION

Lanthanide-doped upconversion nanoparticles (UCNPs) can convert continuous-wave (CW) near-infrared (NIR) excitation to visible emission with a large anti-Stokes shift of several hundred nanometers.[1−3] Compared to the organic dye and inorganic semiconductor nanoparticles, UCNPs have been proved to exhibit superior features, such as no autofluorescence from biological samples, a remarkable light penetration depth, and no photobleaching in bioapplications.[4] As a result, UCNPs are ideal luminescent probes for visualizing living cells and whole-body animals.[5,6] To date, several groups have developed upconversion luminescence (UCL) nanoprobes for small-animal bioimaging *in vivo*. However, most of the reported UCL bioimaging *in vivo* is focused on biodistribution of the UCNPs in different organism, because no recognition unit exists in the UCNPs.

To achieve sensing function, the UCNPs should be combined with other chromophores with recognition sites, through the luminescence resonance energy-transfer (LRET) process. Nowadays, several LRET systems have been developed to detect DNA,[7] special ions,[8] and small molecules[9] in solution, where the UCNPs (donor) transfer energy to the organic chromophores (acceptor) resulting in changes in UCL emission. Compared with the rapid development of UCL solution detection, only three UCL systems combined with both sensing and imaging function to monitor special analytes in cell level have been reported. For example, our group developed an iridium(III) complex-modified UCNP for monitoring intracellular CN^-.[8c] Liu et al. discovered a combination of UCNPs and manganese dioxide nanosheets for the selective detection of glutathione.[9f] Unfortunately, the above-mentioned UCNPs systems were unsuitable to be applied in animal bioimaging. Due to the high affinity of lanthanide ions to some anions (such as PO_4^{3-} and CO_3^{2-}),[10] the chromophore (as energy acceptor) coated on the surface of UCNPs by coordination interaction will disassociate when the chromophore-modified UCNPs are injected into the living animals intravenously. In addition, the responsive UCL emission of the reported LRET systems belongs to the visible region, which limits the application of the reported UCL probes in animal imaging. As a result, no example of UCNPs with both sensing and imaging function to monitor special ions or small molecules within living animals has been reported to date.

In light of the fact that the well-known toxic methylmercury ($MeHg^+$) can be accumulated in the organs of animals,[11,12] we are interested in developing UCL bioimaging of $MeHg^+$ (as an example of special analyte) in living animals. In this present study, we demonstrate an upconversion LRET nanosystem composed of the nanophosphors $NaYF_4$: 20% Yb, 1.6% Er, 0.4% Tm and $MeHg^+$-responsible NIR cyanine dye hCy7 (hCy7-UCNPs, Scheme 1) for UCL monitoring of $MeHg^+$

Received: April 16, 2013
Published: June 13, 2013

   dx.doi.org/10.1021/ja403798m | *J. Am. Chem. Soc.* 2013, 135, 9869−9876

Scheme 1. Schematic Illustration of the Synthesis of UCNPs-hCy7 and Its Sensing to $MeHg^+$ with a Change in UCL Emission

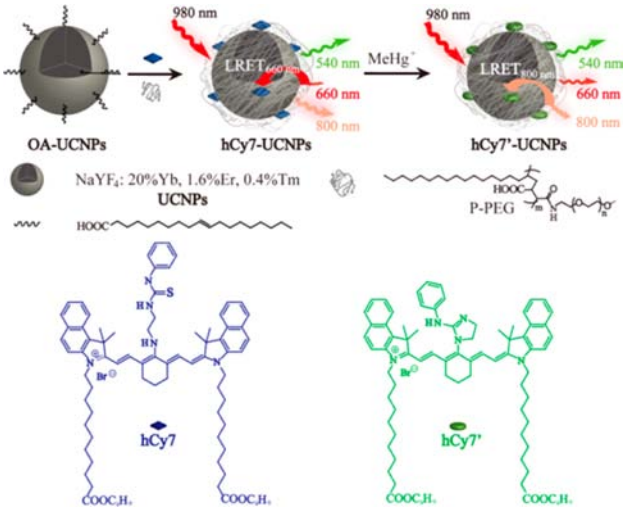

within living small-animal for the first time. The nanoparticles $NaYF_4$: Yb, Er, Tm without and with modification by hCy7 were here abbreviated to UCNPs and hCy7-UCNPs, respectively. Using the ratiometric UCL emission at 800 nm to 660 nm as a detection signal, the detection limit of hCy7-UCNPs for $MeHg^+$ in aqueous solution was as low as 0.18 ppb. Importantly, the hCy7-UCNPs could monitor $MeHg^+$ within the liver and spleen by UCL bioimaging both *ex vivo* and *in vivo*.

RESULTS AND DISCUSSION

Design and Principle of the UCL Nanoprobe for $MeHg^+$. Our design strategy was based on the fact that the lanthanide upconversion nanoparticle has no recognition function but can be used as an energy donor for the LRET process. To achieve a degree of modulating energy transfer (Scheme 2), the emission spectrum of UCNPs and the absorption band of a $MeHg^+$-sensitive chromophore should overlap. As previously reported by Tian et al.,[12] the addition of $MeHg^+$ induced a significant red shift of the maximum absorption peaks of the NIR chemodosimeter Cy7 from 670 to 845 nm. These two absorption band peaks at 845 and 670 nm matched the UCL emissions of $^3H_4 \rightarrow {}^3H_6$ transition (λ_{UCL} = 800 nm) of Tm^{3+} and $^4F_{9/2} \rightarrow {}^4I_{15/2}$ transition (λ_{UCL} = 660 nm) of Er^{3+},[1a] respectively. Thus, it is reasonable that the degree of energy transfer could be modulated by the presence or absence of $MeHg^+$ when Er^{3+} and Tm^{3+}-codoped upconversion nanocrystals ($NaYF_4$: Yb, Er, Tm) and hCy7 are chosen as the energy donor and acceptor, respectively. To combine UCNPs and hCy7 together into one nanosystem, hCy7 was hydrophobized by introducing two long alkyls to match the hydrophobicity of oleic acid (OA)-coated UCNPs, and then both were coated with amphiphilic copolymer through a hydrophobic−hydrophobic interaction. As shown in Scheme 1, a water-soluble three layer structure nanosystem (called hCy7-UCNPs) was composed of an outside hydrophilic layer of PEG, a middle hydrophobic layer containing hydro phobic $MeHg^+$-sensitive hCy7 (as the energy acceptor), and a core of UCNPs and could display both red and NIR UCL emission (as the energy donor).

Scheme 2. Schematic Illustration of the Upconversion LRET Process from the Upconversion Emission of UCNPs to the Absorption of the Dye hCy7 or hCy7′

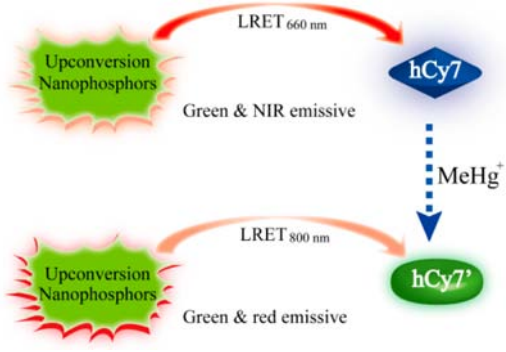

Optical Response of hCy7 to $MeHg^+$. In previous reports,[12] the thiosemicarbazide subunit could sensitively react with $MeHg^+$ to form Cy7′, accompanied by significant changes in photophysical properties. In the present study, the sensing ability of hCy7 for $MeHg^+$ was investigated in EtOH/H_2O (4:1, v/v) by both absorption and fluorescence spectroscopy. The absorption and fluorescence emission spectra of hCy7 in the absence and presence of $MeHg^+$ are shown in Figure 1. The

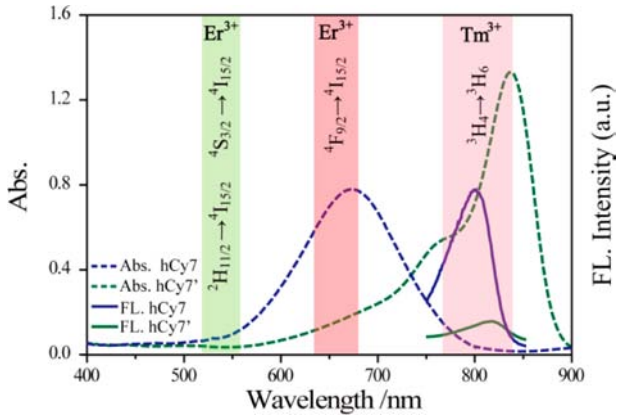

Figure 1. UV−vis absorption (dashes) and photoluminescence (solid) spectra of hCy7 and in the absence and presence of $MeHg^+$ (excitation with 730 nm). The range of main UCL emission bands of Er^{3+} and Tm^{3+} is also shown with different color.

addition of increasing amounts of $MeHg^+$ to a solution of hCy7 induced significant changes in its absorption spectrum. The absorbance at 670 nm ($\varepsilon = 0.9 \times 10^5\ M^{-1}\ cm^{-1}$) decreased gradually, and absorbance at 845 nm ($\varepsilon = 1.5 \times 10^5\ M^{-1}\ cm^{-1}$) gradually increased with an isosbestic point at λ =735 nm, leading to an evident color change from blue to weak green (Figure S4), which indicated a reaction between hCy7 and $MeHg^+$. The isosbestic point at 735 nm clearly showed that only two organic species (free hCy7 and cyclized product hCy7′) coexisted. In the cyclization process, the central bridging secondary amine (N1 atom in Scheme S2) of hCy7 was transformed into the tertiary amine imidazole of hCy7′. The product of the mercury-promoted cyclization reaction was confirmed by MALDI-TOF-MS (Figure S3). The peak at m/z 1194.77 (calculated as 1194.78) was ascribed to hCy7, and the peak at m/z 1160.85 (calculated as 1160.79) was assigned to the cyclized product hCy7′.[12] Furthermore, DFT calculations

dx.doi.org/10.1021/ja403798m | J. Am. Chem. Soc. 2013, 135, 9869−9876

(Figure S5) indicated that this cyclization reaction resulted in a transition of electron donor from the central bridging secondary amine group (N1 atom in Scheme S2) to the indole amine group (N2 atom in Scheme S2), corresponding to the conjugation enhancement in the cyclization product. As a result, a large red-shift in the absorption spectrum with visible color change was observed upon addition of $MeHg^+$ into the hCy7 solution. In addition, at the concentration of hCy7 used in this study, the detection limit of hCy7 for $MeHg^+$ was ~200 ppb.

Moreover, the addition of $MeHg^+$ to hCy7 resulted in a prominent emission change from 800 to 820 nm (Figure 1). Furthermore, the competition experiment[12] indicated that very weak variations in absorption and fluorescence emission of hCy7 were observed after the addition of an excess of other nonmercuric metal ions (Figure S6). These results indicated that hCy7 can serve as a sensitive colormetric and fluorescence indicator for $MeHg^+$.

Synthesis and Characterization of hCy7-UCNPs. In order to fabricate a composite material of UCNPs and hCy7, a polymer-assisted self-assembly method was utilized through a hydrophobic−hydrophobic interaction,[8c,13] and the protocol is represented by Scheme 1. The hexagonal OA-coated UCNPs in diameter of ~25 nm were prepared by the solvothermal method with OA as the surface ligand.[3a,6b] Due to the presence of OA on the surface of the nanoparticles, the OA-UCNPs were hydrophobic. The amphiphilic polymer and hydrophobic hCy7 were cooperatively modified on the surface of the UCNPs (core) to obtain a water-soluble three-layer structure nanosystem of hCy7-UCNPs (Scheme 1). This nanosystem was composed of an outside hydrophilic layer of PEG, a middle hydrophobic layer containing hCy7, and a core of UCNPs.

Transmission electron microscopy (TEM) images indicated no significant changes in size, shape, and crystallinity of UCNPs after modification with hCy7 dye. As shown in Figure 2, the TEM images indicated that both OA-UCNPs and hCy7-UCNPs were uniform with an average diameter of ~25 nm and that no significant aggregates were observed for hCy7-UCNPs after polymer coating. Moreover, the X-ray diffraction peaks of UCNPs correlated well with the hexagonal structure of $NaYF_4$ (JCPDS No.16-0334), which was also confirmed by the high-resolution transmission electron microscopy (HRTEM) image (Figure 2d).

The assembly of the organic dye hCy7 and amphiphilic polymer P-PEG (Scheme 1) on the surface of the UCNPs was investigated by FTIR and ^1H NMR spectra. In the FTIR spectrum of OA-UCNPs (Scheme S8), the bands at 3344 and 1636 cm^{-1} were assigned to OH (asymmetric and symmetric) stretching and δ(C═O), respectively. The bands at 2925 and 2854 cm^{-1} were attributed to asymmetric and symmetric C−H stretching, indicating the presence of OA on the surface of the OA-UCNPs. When compared with the spectrum of OA-UCNPs, new peaks at 1130, 1703, and 1731 cm^{-1} were attributed to the characteristic features of the amides and thiourea groups in the P-PEG and hCy7 appearing in the hCy7-UCNPs (Figure S8),[8c] indicating that the organic hCy7 and P-PEG were successfully assembled on the surface of the nanoparticles by self-assembly. In the ^1H NMR measurement of hCy7-UCNPs (Figure S9), the appearance of the chemical shifts both in the low field assigned to the aromatic protons of hCy7 and in the high field attributed to the protons ($-CH_2-O-$) in the polymer P-PEG[14] demonstrated that the organic dye hCy7 and P-PEG were successfully assembled on the surface of the hCy7-UCNPs (Scheme 1). This indicated that the PEG layer existed outside the surface and hCy7 was successfully doped into the hydrophobic inner layer. By measuring the absorbance at 670 nm with the UV−vis absorption technique, the loading amount of hCy7 on the hydrophobic layer of the hCy7-UCNPs was determined to be ~13.6 wt % (Figure S10), which indicated that hCy7 could be calculated as ~1.66×10^4 units per hCy7-UCNP nanoparticle or ~6.57 units per luminescence center (the total number of Er^{3+} and Tm^{3+} ions).[8b] Moreover, the hCy7-UCNPs showed sufficient stability in water and PBS. In contrast, the loading amount of the two short ethyl chain-modified Cy7 was ~3.4% (Figure S11), much lower than that of the long-chained hCy7. This fact indicated the introduction of the long-chained hCy7 on the surface of UCNPs was important to improve the loading efficiency of $MeHg^+$-response dye.

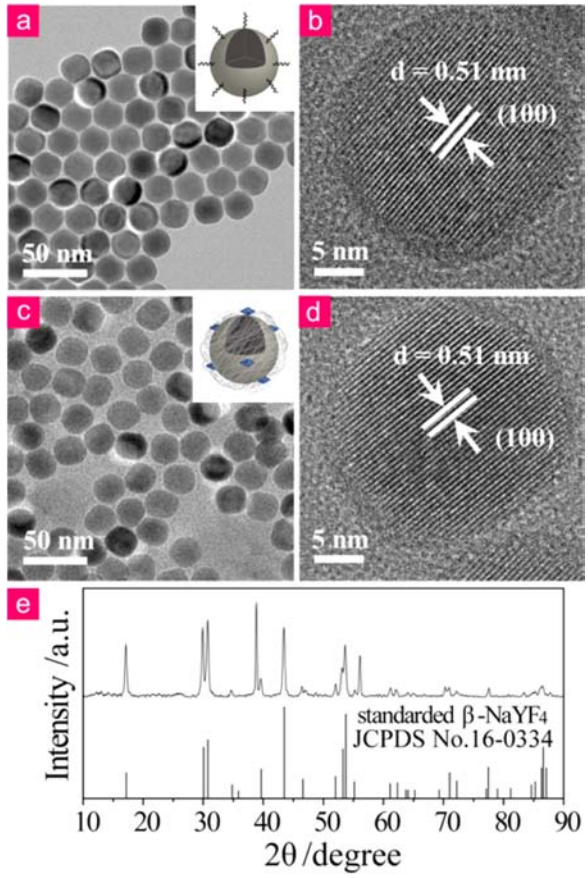

Figure 2. TEM (a) and HR-TEM (b) images of OA-UCNPs. TEM (c) and HR-TEM (d) images of hCy7-UCNPs. (e) X-ray diffraction pattern of UCNPs ($NaYF_4$: 20% Yb, 1.6% Er, 0.4% Tm). The standard pattern of β-$NaYF_4$ (JCPDS no.16-0334) is also shown.

LRET Efficiency. Under CW excitation at 980 nm, the hCy7-UCNPs showed four UCL emission bands at 514−534, 534−560, 635−680, and 800 nm, attributed to the $^2H_{11/2} \rightarrow {}^4I_{15/2}$, $^4S_{3/2} \rightarrow {}^4I_{15/2}$, and $^4F_{9/2} \rightarrow {}^4I_{15/2}$ transitions of Er^{3+} and $^3H_4 \rightarrow {}^3H_6$ transition of Tm^{3+}, respectively,[1a] as illustrated in Figure 3. Compared with the UCL emission spectrum of OA-UCNPs, significant quenching (10-fold) in UCL emission at 635−680 nm was observed for hCy7-UCNPs. The LRET efficiency was measured to be ~90.0%, as deduced from the upconversion emission spectra of hCy7-UCNPs. In contrast, simple physical mixing of OA-UCNPs and hCy7 led to only a

dx.doi.org/10.1021/ja403798m | J. Am. Chem. Soc. 2013, 135, 9869−9876

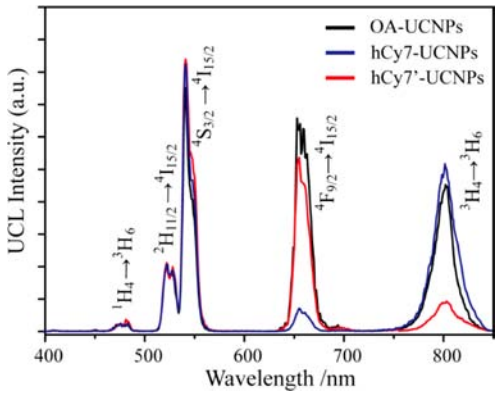

Figure 3. UCL emission spectra of OA-UCNPs, hCy7-UCNPs, and hCy7′-UCNPs under excitation at 980 nm.

0.05-fold decrease in the red emission at 660 nm. These results indicated that the quenching effect in hCy7-UCNPs was mainly ascribed to the LRET process rather than simply absorbed light process by hCy7. Moreover, in the Cy7-UCNPs nanosystem, relative weak quenching in red UCL emission was measured with a LRET efficiency of ∼23% (Figure S11b). These facts indicated that the long-chained hCy7 was necessary to be introduced into upconversion nanosystem to enhance the LRET efficiency.

Sensing of hCy7-UCNPs for $MeHg^+$. The sensing ability of hCy7-UCNPs for $MeHg^+$ was investigated by both UV−vis absorption and UCL emission spectroscopies. In the UV−vis absorption spectrum, the hCy7-UCNPs showed a broad visible band with the maximum absorption wavelength at 670 nm (Figure 4a). Following addition of MeHgCl, this absorption

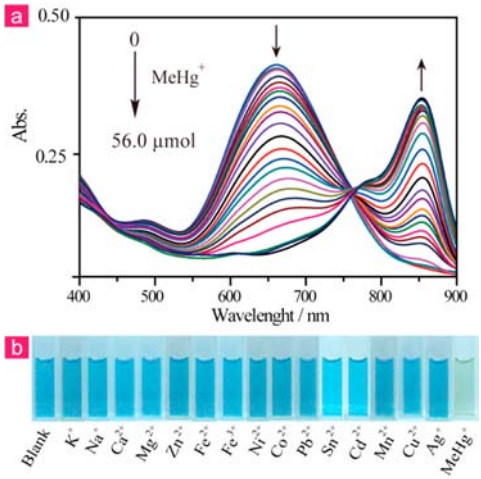

Figure 4. (a) Changed in the absorption spectra of 0.05 mg·mL^{-1} hCy7-UCNPs in the aqueous solution upon gradual addition of $MeHg^+$ ions (from 0 to 8.0 equiv, 56.0 μmol in total). (b) Color change of the aqueous solution of hCy7-UCNPs in the presence of various representative metal ions.

peak was gradually red-shifted from 670 to 845 nm, corresponding to the color change from blue to green (Figure 4b). Such a significant red-shift (∼175 nm) in the absorption band of hCy7-UCNPs following addition of $MeHg^+$ was in agreement with the photophysical change in the pure organic dye hCy7 when interacted with $MeHg^+$ (Figure S4). These findings indicated that a reaction between $MeHg^+$ and the hCy7 in the hydrophobic layer of hCy7-UCNPs existed.

Moreover, this interaction between hCy7-UCNPs and $MeHg^+$ also affected the upconversion emission signals by the LRET process. Following the addition of $MeHg^+$, UCL intensity at 660 nm ($^4F_{9/2} \rightarrow {}^4I_{15/2}$ transition of Er^{3+}) increased significantly, and UCL emission at 800 nm ($^3H_4 \rightarrow {}^3H_6$ transition of Tm^{3+}) decreased for hCy7-UCNPs under excitation at 980 nm (Figure 5a). The UCL emission change

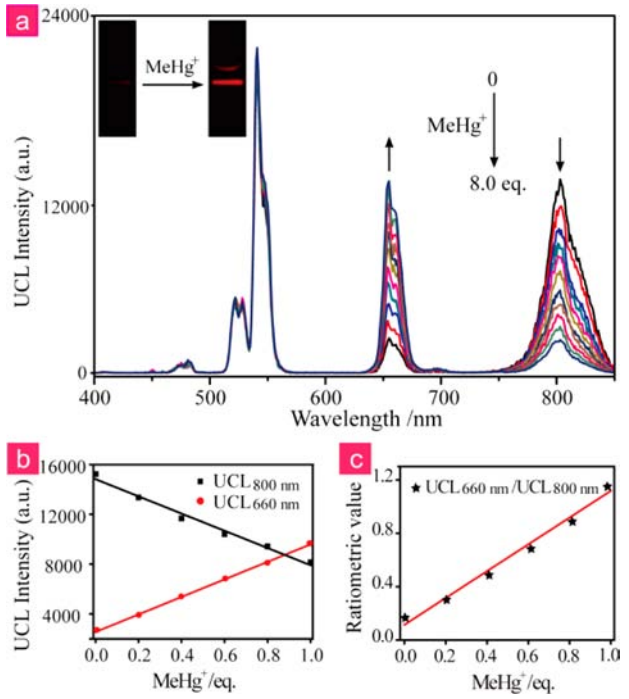

Figure 5. (a) Upconversion luminescence spectra of 0.05 mg·mL^{-1} hCy7-UCNPs in the aqueous solution upon gradual addition of $MeHg^+$ (from 0 to 8 equiv). Inset: the photos showing change in the red UCL emissions. (b) The UCL emissions at 660 ± 2 nm and 800 ± 2 nm as a function of $MeHg^+$ concentration. (c) The ratio of the UCL emission at 660 ± 2 nm to 800 ± 2 nm as a function of $MeHg^+$ concentration.

of hCy7-UCNPs following addition of $MeHg^+$ was attributed to the LRET process. It can be seen from Figure 4 that following the addition of $MeHg^+$, the spectral overlap between the red UCL emission (λ_{em} = 635−680 nm) of UCNPs and absorption (λ_{abs} = 670 nm) of hCy7 was reduced, causing a decrease in the LRET from the red UCL of UCNPs to hCy7. Consequently, the red UCL emissions of hCy7-UCNPs increased in the presence of $MeHg^+$ (Figure 5a). Nevertheless, spectral overlap between the NIR UCL emission (λ_{em} = 800 nm) of UCNPs and absorption (λ_{abs} = 845 nm) of hCy7′ was increased, leading to an increase in the LRET from the NIR UCL of UCNPs to hCy7′. As a result, the NIR UCL emissions of hCy7-UCNPs stopped following the addition of $MeHg^+$ (Figure 5a). Using UCL emission at 800 and 660 nm as detection signals (Figure 5b), the detection limits for $MeHg^+$ in aqueous solution were measured to be ∼0.80 and 0.82 ppb, respectively.

It should be noted that during this interaction process with $MeHg^+$, no significant change in the UCL intensity at 534−560 nm was measured for hCy7-UCNPs, thus the green UCL emission band could be used as the reference standard. Herein, the ratio of UCL intensities at 540, 660, and 800 nm, that is,

dx.doi.org/10.1021/ja403798m | J. Am. Chem. Soc. 2013, 135, 9869−9876

$UCL_{660\ nm}/UCL_{540\ nm}$, $UCL_{800\ nm}/UCL_{540\ nm}$, and $UCL_{660\ nm}/UCL_{800\ nm}$) was also chosen as the detection signals to improve the signal stability and the detection limit. The variation in UCL ratio ($UCL_{660\ nm}/UCL_{540\ nm}$, $UCL_{800\ nm}/UCL_{540\ nm}$, and $UCL_{660\ nm}/UCL_{800\ nm}$) versus the addition of $MeHg^+$ is shown in Figure 5c and Figure S13–S15. Using $UCL_{660\ nm}/UCL_{540\ nm}$, $UCL_{800\ nm}/UCL_{540\ nm}$, and $UCL_{660\ nm}/UCL_{800\ nm}$ as detection signals, the detection limits of hCy7-UCNPs for $MeHg^+$ in aqueous solution were measured to be ~0.58, 0.25, and 0.18 ppb, respectively, which were significantly lower than those when using UCL intensity-based detection (Figure S16–S17). These facts indicated that ratiometric UCL detection is more favorable.

For an excellent chemodosimeter nanosystem, high selectivity and photostability are very important. To validate the selectivity of hCy7-UCNPs, some other metal ions including some alkali (K^+, Na^+), alkaline earth (Ca^{2+}, Mg^{2+}), and transition-metal ions were tested under the same conditions as that of $MeHg^+$ by both absorption and upconversion emission spectroscopy (Figure S18–S19). Only the addition of $MeHg^+$ resulted in a prominent change in absorbance and UCL emission, whereas very weak variations were observed following the addition of an excess of other metal ions (Figure S19). Moreover, competition experiments were carried out by adding $MeHg^+$ to solutions of hCy7-UCNPs in the presence of other cations.[12] In the absence or presence of other cations, significant spectral changes were observed for hCy7-UCNPs following addition of $MeHg^+$ (Figure S20). These results indicated that the sensing of hCy7-UCNPs for $MeHg^+$ was not affected by these common coexistent ions. Therefore, hCy7-UCNPs can act as a highly selective and sensitive ratiometric UCL indicator for $MeHg^+$.

Furthermore, the photostabilities of hCy7-UCNPs under illumination of 980 and 670 nm light were investigated. Under continuous illumination using a 980 nm laser or 670 nm lamp with a power density of 12.6 or 0.3 mW cm^{-2} for 10 h, the absorbance of hCy7-UCNPs at 670 nm decreased by 8.9% and 79.0%, respectively (Figure 6). Therefore, using UCL emission as a detection signal, the hCy7-UCNPs nanosystem showed significant improvement in photostability, which is more useful in practical applications.

Monitoring $MeHg^+$ in Living Cells. Before the application of hCy7-UCNPs in bioimaging, the cytotoxicity of hCy7-UCNPs was investigated by the reduction activity of the methyl thiazolyl tetrazolium (MTT) assay. Following incubation of 100–600 μg mL^{-1} hCy7-UCNPs for 48 h, no significant difference in the proliferation of HeLa and KB cells was observed (Figure S21). After incubation with 500 μg mL^{-1} hCy7-UCNPs for 48 h, the cellular viability of KB and HeLa cells was >85% or 80%, respectively, indicating that the hCy7-UCNPs had low cytotoxicity.

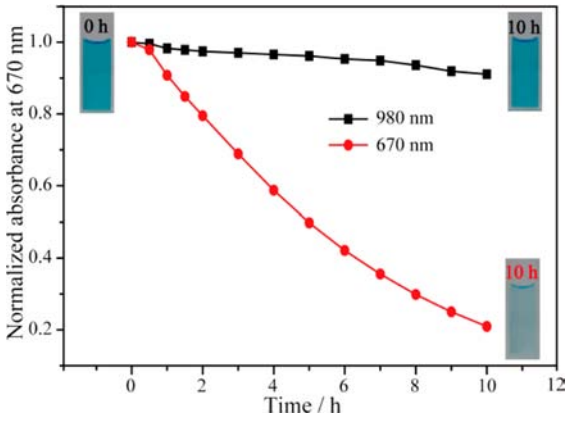

Figure 6. Photostability of hCy7-UCNPs under continuously illumination by 980 nm laser (12.6 mW cm^{-2}) and 670 nm lamp (0.3 mW cm^{-2}) for 10 h.

To demonstrate the applicability of the hCy7-UCNPs in monitoring intracellular $MeHg^+$, laser-scanning upconversion luminescence microscopy (LSUCLM)[4b] experiments were carried out (Figure 7). As determined by LSUCLM, HeLa cells incubated with hCy7-UCNPs (0.05 mg mL^{-1}) for 1 h at 37 °C showed only a weak UCL emission at 660 nm. When the cells were supplemented with 50 μM $MeHg^+$ in the growth medium for 1 h at 37 °C and then incubated with hCy7-UCNPs under the same conditions, a strong enhancement in the red UCL emission was observed in the intracellular region. Bright-field measurements confirmed that the HeLa cells with or without treatment with $MeHg^+$ remained viable throughout the imaging experiments. Furthermore, in light of the rapid enhancement of red UCL at 660 nm over green UCL at 540 nm of hCy7-UCNPs when interacted with $MeHg^+$, the ratiometric UCL imaging was further investigated.

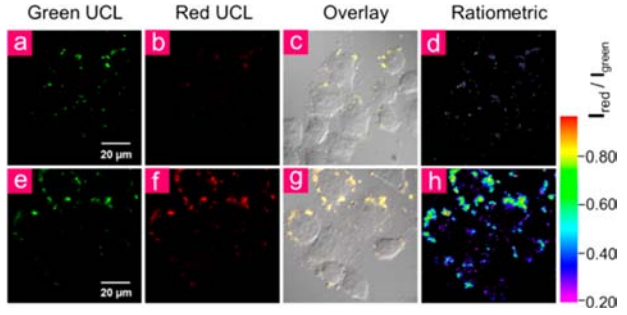

Figure 7. Ratiometric UCL images in living HeLa cells (top, a–d) and 50 μM $MeHg^+$-pretreated Hela Cells (bottom, e–h) incubated with 0.05 mg mL^{-1} hCy7-UCNPs for 2 h at 37 °C. Emission was collected by green UCL channel at 500–560 nm (a and e) and red channel at 600–700 nm (b and f), under excitation at 980 nm. (c and g) Overlay of bright-field, green and red UCL imagings. (d and h) Ratiometric UCL images with ratio of red to green channels.

The UCL ratio at the red channel (λ_{UCL} = 600–700 nm) to green channel (λ_{UCL} = 500–560 nm) was used as the detection signal. As shown in Figure 7d, HeLa cells incubated with hCy7-UCNPs (0.05 mg mL^{-1}) for 2 h at 37 °C showed a UCL ratio <0.4. Following incubation of $MeHg^+$-pretreated HeLa cells with hCy7-UCNPs (0.05 mg mL^{-1}), the corresponding UCL ratio was increased to 0.8 (Figure 7h). These results suggested that hCy7-UCNPs could be used for monitoring intracellular $MeHg^+$ with the ratiometric UCL method.

UCL Monitoring *in Vivo* of $MeHg^+$. The *in vivo* accumulation of $MeHg^+$ is related to the development of visceral injury, especially liver injury in mammals. As previously reported, lanthanide UCNPs were enriched in the livers of living mice following intravenous injection.[1f] Herein, the hCy7-UCNPs nanosystem was further investigated to monitor $MeHg^+$ in a mouse model. Male Kunming mice (4 weeks old, ~20 g) were injected intravenously with hCy7-UCNPs (0.2 mL, 0.2 mg·mL^{-1} in physiological saline) and divided into two equal groups. As shown in Figure 8, the left group (control

dx.doi.org/10.1021/ja403798m | J. Am. Chem. Soc. 2013, 135, 9869–9876

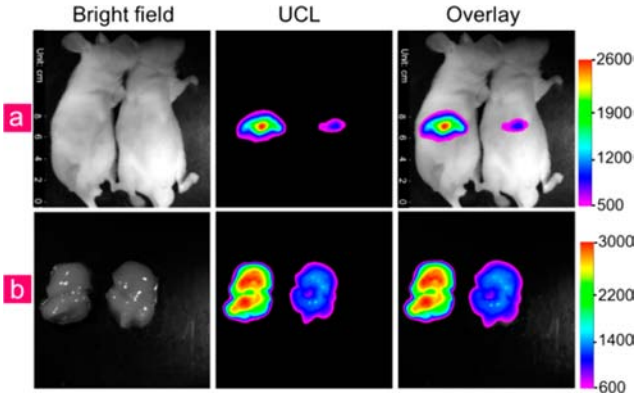

Figure 8. (a) *In vivo* UCL images of 40 μg hCy7-UCNPs-pretreated living mice injected intravenously with 0.2 mL normal saline (left mouce) or 0.1 mM $MeHg^+$ solution (right mouse). (b) The corresponding UCL images of the livers which were isolated from the above dissected mice. The UCL emission was collected at 800 ± 12 nm upon irradiation at 980 nm.

group) was injected intravenously with physiological saline (0.2 mL), and the right group was injected intravenously with $MeHg^+$ (0.2 mL, 0.1 mM) in saline.

UCL imaging *in vivo* indicated that the hCy7-UCNPs mainly accumulated in the livers of mice (Figure 8). Compared with control mice treated with normal saline, the UCL at 800 nm decreased to 50% of the original value after treatment with $MeHg^+$ (Figure 8a). The mice in the two groups were subsequently dissected to isolate the livers. The UCL emission in the liver of $MeHg^+$-pretreated mice was weaker than that in the control mice (Figure 8b). Furthermore, the livers of normal mice were divided into small pieces in another experiment, which were then immersed in $MeHg^+$ solution or in saline for different time periods. As shown in Figure 9, the UCL intensity at 800 nm in the $MeHg^+$-pretreated group decreased with

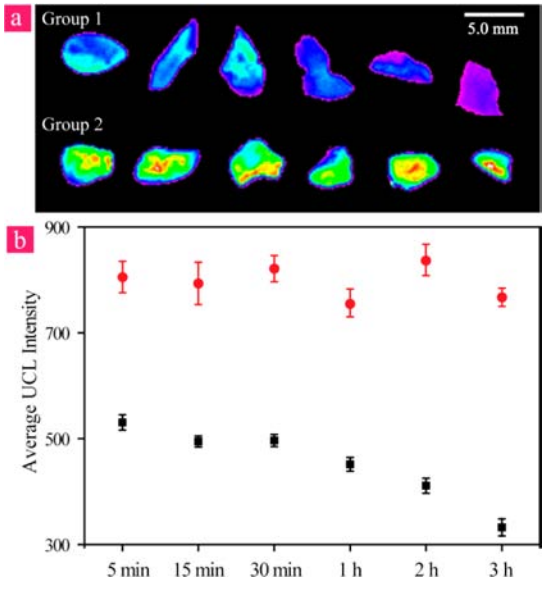

Figure 9. UCL imaging (a) and the corresponding change in average UCL intensity (b) of the hCy7-UCNPs-pretreated livers which were immersed with 0.1 mM $MeHg^+$ solution (Group 1) or saline (Group 2) for different times (5, 15, and 30 min and 1, 2, and 3 h). The UCL emission was collected at 800 ± 12 nm upon irradiation at 980 nm.

increasing incubation time, and no significant change in the control group was observed. These findings indicated that the nanosystem (hCy7-UCNPs) could effectively detect $MeHg^+$ both *ex vivo* and *in vivo*.

CONCLUSION

In summary, we have demonstrated a highly sensitive water-soluble nanosystem based on cyanine dye-assembled nanophosphors for UCL sensing and bioimaging of $MeHg^+$ ions. The cyanine dye hCy7, a $MeHg^+$-sensitive dye, was successfully assembled on the surface of lanthanide UCNPs. This dye-assembled nanosystem could be used for ratiometric UCL detection of $MeHg^+$ in aqueous solution with high sensitivity (detection limit of 0.18 ppb). This detection limit was lower than the blood level (5.8 ppb) set by the U.S. EPA. Importantly, the nanosystem was capable of monitoring $MeHg^+$ in living cells and small animals by UCL bioimaging. Our successful ratiometric UCL-based nanosystem for sensing and bioimaging $MeHg^+$ provides a new design strategy for further novel probes for highly sensitive *in vivo* bioimaging studies.

MATERIALS AND INSTRUMENTS

Materials. All reagents and chemicals were purchased from commercial sources and used without further purification. 2,3,3-Trimethylbenzoindolenine, 10-bromoundecanoic acid, phenyl-4-isothiocyanate, OA, 1-octadecane (ODE 90%), 1,2-dichlorobenzene, $POCl_3$, cyclohexanone, *n*-butanol, ethylenediamine, and benzene were obtained from Alfa Aesar Ltd. Rare earth oxides Y_2O_3 (99.999%), Yb_2O_3 (99.999%), Er_2O_3 (99.999%), and Tm_2O_3 (99.999%) were purchased from Shanghai Yuelong New Materials Co. Ltd. $RECl_3$ (RE^{3+} = Y^{3+}, Yb^{3+}, Er^{3+}, and Tm^{3+}) were prepared with the literature method.[15] DMF and deionized water was used to prepare all aqueous solutions. Solutions of $MeHg^+$, Cu^{2+}, Zn^{2+}, and Fe^{2+} ions were prepared from their chlorate salts, and solutions of Ag^+, Ni^{2+}, Cd^{2+}, Pb^{2+}, and Co^{2+} were prepared from their nitrate salts. The amphiphilic block-polymer poly(maleic anhydride-alt-1-octadecene)-PEG (P-PEG) was prepared according to the previous literatures.[14] The intermediates, 1*H*-Benz[*e*]indolium, 3-(10-carboxydecyl)-1,1,2-trimethyl bromide (2),[16] 2-chilor-1-formy-3-(hydroxymenthylene)-cyclohex-1-ene (4),[17] and subside thiourea derivative (7),[18] were prepared according to the previous literatures.

Characterization. The ^1H NMR spectra were recorded on a Bruker spectrometer at 400 MHz. All chemical shifts are reported in the standard δ notation of parts per million. Electrospray ionization mass spectra were measured on a Micromass LCTTM system. UV−vis absorption spectra were recorded on a Shimadzu 3000 spectrophotometer. UCL emission spectra were measured on an Edinburgh FLS920 luminescence spectrometer with an external 3 W adjustable 980 nm semiconductor laser (Beijing Hi-Tech Optoelectronic Co., China). In our case, all power densities of CW 980 nm excitation for the UCL measurements were fixed at 45 W cm^{-2}. FT-IR spectra were measured using an IR Prestige-21 spectrometer (Shimadzu) from samples in KBr pellets. X-ray powder diffraction measurements were performed on a Bruker D_8 diffractometer at a scanning rate of 1° min^{-1} in the 2θ range of 10−90°, with graphite monochromated Cu K_α radiation (λ = 1.5406 nm). TEM images were collected on a JEM 2010 operating at an acceleration voltage of 200 kV. The as-prepared samples were dispersed in cyclohexane and dripped onto a copper grid for the TEM tests.

Synthesis of OA-UCNPs. OA-UCNPs were prepared by a modified solvothermal process according to the reported method.[3a,6b] YCl_3 (0.78 mmol), $YbCl_3$ (0.20 mmol), $ErCl_3$ (0.016 mmol), and $TmCl_3$ (0.004 mmol) were mixed with 6 mL OA and 15 mL ODE in a 50 mL flask. The solution was heated to 160 °C to form a homogeneous solution and then cooled down to room temperature. Eight mL methanol solution containing NaOH (2.5 mmol) and NH_4F

dx.doi.org/10.1021/ja403798m | J. Am. Chem. Soc. 2013, 135, 9869−9876

(4 mmol) was slowly added into the flask and stirred for 30 min. Subsequently, the solution was slowly heated and degassed at 120 °C for 10 min to remove methanol and then heated to 300 °C and maintained for 1 h under Ar protection. After the solution was cooled naturally, nanoparticles were precipitated from the solution with ethanol and washed with ethanol/cyclohexane (9:1, v/v) for three times.

Synthesis of hCy7. The synthetic routine of the dye hCy7 is shown in the Scheme S1.

Compound 5. Into a flask attached with Dean−Stark trap and a condenser were added freshly prepared 2-chloro-1-formyl-3-(hydroxymethylene)cyclohex-1-ene 4 (1.7 g, 10 mmol), 1*H*-Benz[*e*]-indolium, 3-(10-carboxydecyl)-1,1,2-trimethyl-, bromide 2 (7.9 g, 20 mmol), *n*-butanol (200 mL), and benzene (20 mL). The mixture was heated to 120 °C for 24h, resulting in a green solution. Solvents were removed on a rotavapor. Residue was washed with hexane/EtOAc and eluted with DCM/MeOH from a silica gel plug to give the crude product. Further chromatography on a silica gel column with gradient DCM/MeOH solvent system led to 14.7 g (60%) of 5 as dark-green solid. ^{1}H NMR (400 MHz, $CDCl_3$) δ 8.47 (d, J = 14.2 Hz, 2H), 8.15 (d, J = 8.5 Hz, 2H), 7.99−7.96 (m, 4H), 7.66−7.61 (m, 2H), 7.52−17.46 (m, 4H), 6.30 (d, J = 14.2 Hz, 2H), 4.35 (t, J = 7.2 Hz, 4H), 4.07 (t, J = 6.7 Hz, 4H), 2.79 (t, J = 5.9 Hz, 4H), 2.28 (t, J = 7.5 Hz, 4H), 2.04 (s, 12H), 1.97−1.88 (m, 4H), 1.64−1.56 (m, 8H), 1.53−1.46 (m, 4H), 1.43−1.34 (m, 8H), 1.33−1.21 (m, 18H), 0.93 (t, J = 7.4 Hz, 6H). MS (MALDI-TOF-MS): calcd for $C_{68}H_{92}ClN_2O_4^+$, 1035.67 $[M]^+$; found, 1035.10 $[M]^+$.

Compound hCy7. Subside thiourea derivative 7 (0.39 g, 2.0 mmol) and compound 5 (1.11 g, 1.0 mmol) were dissolved in anhydrous DMF (50 mL). The mixture was stirred at 85 °C for 12 h under an argon atmosphere. The solvent was removed under reduced pressure, and then the crude product was purified by silica gel chromatography with DCM/MeOH (30:1) to afford the desired product as a deep-blue solid (40%). ^{1}H NMR (400 MHz, $CDCl_3$) δ 10.08 (br, 1H), 9.63 (br, 1H), 8.57 (br, 1H), 7.95 (d, J = 8.4 Hz, 2H), 7.90−7.80 (m, 3H), 7.78 (d, J = 12.7 Hz, 2H), 7.50 (t, J = 8.0 Hz 2H), 7.36 (t, J = 8.0 Hz 2H), 7.32 (t, J = 8.0 Hz 2H), 7.16 (d, J = 8.7 Hz, 2H), 7.11 (t, J = 8.0 Hz 1H), 5.62 (d, J = 13.0 Hz, 2H), 4.13−4.05 (m, 8H), 3.91−3.85 (m, 4H), 2.52 (t, J = 5.8 Hz, 4H), 1.94 (s, 12H), 1.91−1.85 (m, 2H), 1.82−1.75 (m, 4H), 1.44−1.32 (m, 40H), 0.92 (t, J = 7.3 Hz, 6H); MS (MALDI-TOF-MS): calcd for $C_{77}H_{104}N_5O_4S^+$, 1194.74 $[M]^+$; found, 1194.77 $[M]^+$.

Assembly of P-PEG and hCy7 (denoted as hCy7-UCNPs). hCy7-UCNPs were prepared according to the previous method.[8c] The UCNPs (10 mg) and hCy7 (5 mg) were dispersed in the 5 mL chloroform by ultrasonication, and then the mixture was stirred at room temperature to obtain a homogeneous phase. Furthermore, the amphiphilic polymer (P-PEG, 10 mg) was added, and then the mixture was stirred overnight at room temperature. The mixture was centrifugated (14000 rpm, 8 min every time in 20 °C), and the collected solid was repeatedly washed with water. The precipitate could be redispersed in deionized water.

Procedures for Cation Titration. Stock solutions of the metal ions (2.5 mM) were prepared in H_2O. A stock solution of hCy7-UCNPs (containing 10 μM hCy7) was prepared in H_2O. The sensing of hCy7-UCNPs to $MeHg^+$ was performed by adding the $MeHg^+$ stock solution by means of a micropipet to 2 mL solution of hCy7-UCNPs. Test samples for selectivity experiments were prepared by adding appropriate amounts of anions stock solution with a similar procedure. In competition experiments, $MeHg^+$ was added to solutions containing hCy7-UCNPs and the other metal ions of interest. All test solutions were stirred for 20 min at room temperature. For all UCL measurements, excitation was fixed at 980 nm, and UCL emission was collected from 400 to 850 nm.

Cell Culture. The cell lines HeLa and KB were provided by the Institute of Biochemistry and Cell Biology, SIBS, CAS (China). The HeLa and KB cells were grown in modified Eagle's medium supplemented with 10% fetal bovine serum at 37 °C and 5% CO_2. HeLa and KB cells were planted on 14 mm glass coverslips and allowed to adhere for 24 h.

Cytotoxicity of hCy7-UCNPs. *In vitro* cytotoxicity was measured by performing MTT assays on the HeLa and KB cells. Cells were seeded into a 96-well cell culture plate at 5×10^4/well, under 100% humidity, and were cultured at 37 °C and 5% CO_2 for 24 h; different concentrations of hCy7-UCNPs (0, 100, 200, 300, 400, 500, and 600 μg/mL, diluted in RPMI 1640) were then added to the wells. The cells were subsequently incubated for 24 or 48 h at 37 °C under 5% CO_2. Then, MTT (10 mL; 5 mg/mL) was added to each well, and the plate was incubated for an additional 4 h at 37 °C under 5% CO_2. After the addition of 100 μL DMSO, the assay plate was allowed to stand at room temperature for 2 h. The optical density OD570 value (Abs) of each well, with background subtraction at 690 nm, was measured by means of a Tecan Infinite M200 monochromator-based multifunction microplate reader.[19] The following formula was used to calculate the inhibition of cell growth:

$$\text{cell viability}(\%) = (\text{mean Abs value of treatment group} / \text{mean Abs value of control}) \times 100\%$$

LSUCLM Imaging. Experiment to assess $MeHg^+$ uptake was performed over 1 h in the same medium supplemented with 50 μM $MeHg^+$. Before the experiments, HeLa cells were washed with PBS buffer for three times, and then the cells were incubated with 5 μM hCy7-UCNPs in PBS for 1 h at 37 °C. Cell imaging was then carried out after washing the cells with PBS. LSUCLM imaging was performed with an OLYMPUS FV1000 scanning unit.[4b] Cells loaded with hCy7-UCNPs were excited by a CW laser at 980 nm (Connet Fiber Optics, China) with the focused power of ∼14 mW. UCL emission was collected at 500−560 and 600−700 nm.

Upconversion Luminescence *In Vivo* Imaging. Animal procedures were in agreement with the guidelines of the Institutional Animal Care and Use Committee. *In vivo* and *ex vivo* UCL imaging was performed with a modified upconversion luminescence *in vivo* imaging system designed by our group.[4c] In this system, two external 0−5 W adjustable CW 980 nm lasers (Connet Fiber Optics, China) and an Andor DU897 EMCCD were used as the excitation sources and the signal collector, respectively. Images of luminescent signals were analyzed with Kodak Molecular Imaging Software. UCL signals were collected at 800 ± 12 nm with a bandpass filter (Semrock).

■ ASSOCIATED CONTENT

Supporting Information

The synthetic details, ^{1}H NMR, MADLI-TOF MS, FT-IR, EDXA spectra, and cell viability of hCy7-UCNPs. The changes of UV−vis absorption and UCL emission spectra in various $MeHg^+$. This material is available free of charge via the Internet at http://pubs.acs.org.

■ AUTHOR INFORMATION

Corresponding Author

fyli@fudan.edu.cn

Notes

The authors declare no competing financial interest.

■ ACKNOWLEDGMENTS

The authors thank National Science Foundation of China (21231004 and 91027004), MOST of China (2011AA03A407 and 2012CB932403), Shanghai Sci. Tech. Comm. (11XD1400200 and 12JC1401300), and the innovative team of Ministry of Education of China (IRT0911) for financial support.

■ REFERENCES

(1) (a) Auzel, F. *Chem. Rev.* **2004**, *104*, 139. (b) Feng, W.; Sun, L. D.; Zhang, Y. W.; Yan, C. H. *Coord. Chem. Rev.* **2010**, *254*, 1038. (c) Mader, H. S.; Kele, P.; Saleh, S. M.; Wolfbeis, O. S. *Curr. Opin.*

Chem. Biol. **2010**, *14*, 582. (d) Wang, G. F.; Peng, Q.; Li, Y. D. *Acc. Chem. Res.* **2011**, *44*, 322. (e) Schäfer, H.; Haase, M. *Angew. Chem., Int. Ed.* **2011**, *50*, 5808. (f) Zhou, J.; Liu, Z.; Li, F. Y. *Chem. Soc. Rev.* **2012**, *41*, 1323.

(2) (a) Liu, Y. S.; Tu, D. T.; Zhu, H. M.; Li, R. F.; Luo, W. Q.; Chen, X. Y. *Adv. Mater.* **2010**, *22*, 3266. (b) Wang, F.; Han, Y.; Lim, C. S.; Lu, Y. H.; Wang, J.; Xu, J.; Chen, H. Y.; Zhang, C.; Hong, M. H.; Liu, X. G. *Nature* **2010**, *463*, 1061. (c) Wang, F.; Deng, R. R.; Wang, J.; Wang, Q. X.; Han, Y.; Zhu, H. M.; Chen, X. Y.; Liu, X. G. *Nat. Mater.* **2011**, *10*, 968. (d) Su, Q. Q.; Han, S. Y.; Xie, X. J.; Zhu, H. M.; Chen, H. Y.; Chen, C.-K.; Liu, R.-S.; Chen, X. Y.; Wang, F.; Liu, X. G. *J. Am. Chem. Soc.* **2012**, *134*, 20849. (e) Mai, H. X.; Zhang, Y. W.; Si, R.; Yan, Z. G.; Sun, L. D.; You, L. P.; Yan, C. H. *J. Am. Chem. Soc.* **2006**, *128*, 6426. (f) Wu, S. W.; Han, G.; Milliron, D. J.; Aloni, S.; Altoe, V.; Talapin, D. V.; Cohen, B. E.; Schuck, P. J. *Proc. Natl. Acad. Sci.U.S.A.* **2009**, *106*, 10917. (g) Jalil, R. A.; Zhang, Y. *Biomaterials* **2008**, *29*, 4122. (h) Xu, Z. H.; Ma, P. A.; Li, C. X.; Hou, Z. Y.; Zhai, X. F.; Huang, S. S.; Lin, J. *Biomaterials* **2011**, *32*, 4161. (i) Abel, K. A.; Boyer, J. C.; van Veggel, F. C. J. M. *J. Am. Chem. Soc.* **2009**, *131*, 14644. (j) Yan, B.; Boyer, J. C.; Habault, D.; Branda, N. R.; Zhao, Y. *J. Am. Chem. Soc.* **2012**, *134*, 16558. (k) Jayakumar, M. K. G.; Idris, N. M.; Zhang, Y. *Proc. Natl. Acad. Sci. U.S.A.* **2012**, *109*, 8483.

(3) (a) Liu, Q.; Sun, Y.; Li, C. G.; Zhou, J.; Li, C. Y.; Yang, T. S.; Zhang, X. Z.; Yi, T.; Wu, D. M.; Li, F. Y. *ACS Nano* **2011**, *5*, 3146. (b) Xiong, L. Q.; Chen, Z. G.; Yu, M. X.; Li, F. Y.; Liu, C.; Huang, C. H. *Biomaterials* **2009**, *30*, 5592. (c) Liu, Q.; Yin, B. R.; Yang, T. S.; Yang, Y. C.; Shen, Z.; Yao, P.; Li, F. Y. *J. Am. Chem. Soc.* **2013**, *135*, 5029. (d) Sun, Y.; Liu, Q.; Peng, J. J.; Zhou, J.; Yang, P. Y.; Zhang, Y. J.; Li, F. Y. *Biomaterials* **2013**, *34*, 2289.

(4) (a) Chatteriee, D. K.; Rufalhah, A. J.; Zhang, Y. *Biomaterials* **2008**, *29*, 937. (b) Yu, M. X.; Li, F. Y.; Chen, Z. G.; Hu, H.; Zhan, C.; Yang, H.; Huang, C. H. *Anal. Chem.* **2009**, *81*, 930. (c) Xiong, L. Q.; Chen, Z. G.; Tian, Q. W.; Cao, T. Y.; Xu, C. J.; Li, F. Y. *Anal. Chem.* **2009**, *81*, 8687. (d) Liu, Q.; Sun, Y.; Yang, T. S.; Feng, W.; Li, C. G.; Li, F. Y. *J. Am. Chem. Soc.* **2011**, *133*, 17122. (e) Liu, Q.; Yang, T. S.; Feng, W.; Li, F. Y. *J. Am. Chem. Soc.* **2012**, *134*, 5390.

(5) (a) Zhou, J. C.; Yang, Z. L.; Dong, W.; Tang, R. J.; Sun, L. D.; Yan, C. H. *Biomaterials* **2011**, *32*, 9059. (b) Xing, H. Y.; Bu, W. B.; Zhang, S. J.; Zheng, X. P.; Li, M.; Chen, F.; He, Q. J.; Zhou, L. P.; Peng, W. J.; Hua, Y. Q.; Shi, J. L. *Biomaterials* **2012**, *33*, 1079. (c) Boyer, J. C.; Manseau, M. P.; Murray, J. I.; van Veggel, F. C. J. M. *Langmuir* **2010**, *26*, 1157. (d) Cheng, L.; Yang, K.; Li, Y. G.; Chen, J. H.; Wang, C.; Shao, M. W.; Lee, S. T.; Liu, Z. *Angew. Chem., Int. Ed.* **2011**, *50*, 7385. (e) Cheng, L.; Yang, K.; Shao, M. W.; Lee, S. T.; Liu, Z. *J. Phys. Chem. C* **2011**, *115*, 2686. (f) Hilderbrand, S. A.; Shao, F. W.; Salthouse, C.; Mahmood, U.; Weissleder, R. *Chem. Commun.* **2009**, 4188.

(6) (a) Zhou, J.; Sun, Y.; Du, X. X.; Xiong, L. Q.; Hu, H.; Li, F. Y. *Biomaterials* **2010**, *31*, 3287. (b) Liu, Q.; Chen, M.; Sun, Y.; Chen, G. Y.; Yang, T. S.; Gao, Y.; Zhang, X. Z.; Li, F. Y. *Biomaterials* **2011**, *32*, 8243. (c) Zhou, J.; Yu, M. X.; Sun, Y.; Zhang, X. Z.; Zhu, X. J.; Wu, Z. H.; Wu, D. M.; Li, F. Y. *Biomaterials* **2011**, *32*, 1148. (d) Xia, A.; Chen, M.; Gao, Y.; Wu, D. M.; Feng, W.; Li, F. Y. *Biomaterials* **2012**, *33*, 5394. (e) Zhu, X. J.; Zhou, J.; Chen, M.; Shi, M.; Feng, W.; Li, F. Y. *Biomaterials* **2012**, *33*, 4618.

(7) (a) Chen, Z. G.; Chen, H. L.; Hu, H.; Yu, M. X.; Li, F. Y.; Zhang, Q.; Zhou, Z. G.; Yi, T.; Huang, C. H. *J. Am. Chem. Soc.* **2008**, *130*, 3023. (b) Kumar, M.; Zhang, P. *Langmuir* **2009**, *25*, 6024. (c) Jiang, S.; Zhang, Y. *Langmuir* **2010**, *26*, 6689. (d) Zhang, F.; Shi, Q. H.; Zhang, Y. C.; Shi, Y. F.; Ding, K. L.; Zhao, D. Y.; Stucky, G. D. *Adv. Mater.* **2011**, *23*, 3775. (e) Rantanen, T.; Pakkila, H.; Jamsen, L.; Kuningas, K.; Ukonaho, T.; Lovgren, T.; Soukka, T. *Anal. Chem.* **2007**, *79*, 6312. (f) Rantanen, T.; Jarvenpaa, M. L.; Vuojola, J.; Kuningas, K.; Soukka, T. *Angew. Chem., Int. Ed.* **2008**, *47*, 3811. (g) Zhang, P.; Rogelj, S.; Nguyen, K.; Wheeler, D. *J. Am. Chem. Soc.* **2006**, *128*, 12410.

(8) (a) Liu, J. L.; Liu, Y.; Liu, Q.; Li, C. Y.; Sun, L. N.; Li, F. Y. *J. Am. Chem. Soc.* **2011**, *133*, 15276. (b) Liu, Q.; Peng, J. J.; Sun, L. N.; Li, F. Y. *ACS Nano* **2011**, *5*, 8040. (c) Yao, L. M.; Zhou, J.; Liu, J. L.; Feng, W.; Li, F. Y. *Adv. Funct. Mater.* **2012**, *22*, 2667. (d) Xie, L.; Qin, Y.; Chen, H.-Y. *Anal. Chem.* **2012**, *84*, 1969. (e) Li, C. X.; Liu, J. L.; Alonso, S.; Li, F. Y.; Zhang, Y. *Nanoscale* **2012**, *4*, 6065.

(9) (a) Ali, R.; Saleh, S. M.; Meier, R. J.; Azab, H. A.; Abdelgawad, I. I.; Wolfbeis, O. S. *Sens. Actuators, B* **2010**, *150*, 126. (b) Mader, H. S.; Wolfbeis, O. S. *Anal. Chem.* **2010**, *82*, 5002. (c) Achatz, D. E.; Meier, R. J.; Fischer, L. H.; Wolfbeis, O. S. *Angew. Chem., Int. Ed.* **2011**, *50*, 260. (d) Fischer, L. H.; Harms, G. S.; Wolfbeis, O. S. *Angew. Chem., Int. Ed.* **2011**, *50*, 4546. (e) Sun, L. N.; Peng, H. S.; Stich, M. I. J.; Achatz, D.; Wolfbeis, O. S. *Chem. Commun.* **2009**, 5000. (f) Deng, R. R.; Xie, X. J.; Vendrell, M.; Chang, Y. T.; Liu, X. G. *J. Am. Chem. Soc.* **2011**, *133*, 20168.

(10) *Coordination Chemistry of Rare Earth Complexes*; Huang, C. H., Ed.; Science Press: Beijing, 1997.

(11) (a) Zalups, R. K.; Lash, L. H. *Toxicol. Appl. Pharmacol.* **2006**, *214*, 88. (b) Ando, S.; Koide, K. *J. Am. Chem. Soc.* **2011**, *133*, 2556. (c) Yang, Y. K.; Yook, K. J.; Tae, J. *J. Am. Chem. Soc.* **2005**, *127*, 16760. (d) Yang, Y. M.; Zhao, Q.; Feng, W.; Li, F. Y. *Chem. Rev.* **2013**, *113*, 192. (e) Chen, X. Q.; Baek, K. H.; Kim, Y. M.; Kim, S. J.; Shin, I.; Yoon, J. Y. *Tetrahedron* **2010**, *66*, 4016. (f) Chan, D. S.-H.; Lee, H.-M.; Che, C.-M.; Leung, C.-H.; Ma, D.-L. *Chem. Commun.* **2009**, 7479. (g) He, H.-Z.; Leung, K.-H.; Fu, W.-C.; Chan, D. S.-H.; Leung, C.-H.; Ma, D.-L. *Environ. Res. Lett.* **2012**, *7*, 044032 (7pp).

(12) Guo, Z. Q.; Zhu, W. H.; Zhu, M. M.; Wu, X. M.; Tian, H. *Chem.—Eur. J.* **2010**, *16*, 14424.

(13) Wang, C.; Cheng, L.; Liu, Z. *Biomaterials* **2011**, *32*, 1110.

(14) Prencipe, G.; Tabakman, S. M.; Welsher, K.; Liu, Z.; Goodwin, A. P.; Zhang, L.; Henry, J.; Dai, H. J. *J. Am. Chem. Soc.* **2009**, *131*, 4783.

(15) Li, Z. Q.; Wang, L. M.; Wang, Z. Y.; Liu, X. G.; Xiong, Y. J. *J. Phys. Chem. C* **2011**, *115*, 3291.

(16) Zhang, Z.; Achilefu, S. *Org. Lett.* **2004**, *6*, 2067.

(17) Reynolds, G. A.; Drexhage, K. H. *J. Org. Chem.* **1977**, *42*, 885.

(18) Yu, M. X.; Shi, M.; Chen, Z. G.; Li, F. Y.; Li, X. X.; Gao, Y. H.; Xu, J.; Yang, H.; Zhou, Z. G.; Yi, T.; Huang, C. H. *Chem.—Eur. J.* **2008**, *14*, 6892.

(19) Li, C. Y.; Yu, M. X.; Sun, Y.; Wu, Y. Q.; Huang, C. H.; Li, F. Y. *J. Am. Chem. Soc.* **2011**, *133*, 11231.